Analysis and reduction of the spurious current in a class of multiphase lattice Boltzmann models

Xiaowen Shan*
Exa Corporation, 3 Burlington Woods Drive, Burlington, Massachusetts 01803, USA
(Received 20 December 2005; published 6 April 2006)

We show that the spurious current present near a curved interface in a class of multiphase lattice Boltzmann (LB) models is due to the insufficient isotropy of the discrete gradient operator. A method of obtaining highly isotropic gradient operators on a lattice is given. Numerical simulations show that both the magnitude and the spatial extent of the spurious current are significantly reduced as gradient operators of increasingly higher order of isotropy is adopted in multiphase LB models.

DOI: 10.1103/PhysRevE.73.047701 PACS number(s): 47.11.−j, 47.55.−t, 05.20.Dd

The lattice Boltzmann (LB) equation method [1,2] is in essence a kinetic theory based computation method for fluid simulations. Some of the microscopic physics giving rise to the complex behavior at macroscopic level can be modeled within the framework of the governing equations owing to its kinetic nature. One example is the modeling of a nonideal gas fluid in the LB equation through a mean-field interaction potential [3,4], which at macroscopic level yields a nonideal gas equation of state and the associated behaviors of multiphase flow and phase transitions. Since its creation, the multiphase LB model has been used in simulations of a wide range of scientific and engineering problems [5–8].

A phenomenon known as the *spurious current* was first discovered in an early LB multiphase model [9] as a small but finite amplitude circulating flow near the interface of a stationary bubble. The flow pattern was found to posses the same symmetry as the underlying lattice and the magnitude of the velocity scales with the surface tension and the inverse of the viscosity. Similar flow pattern was found in the subsequent LB model for nonideal gases and multiple components [3,4] although both the magnitude and the spatial extent of the spurious velocity are much reduced [10].

Before further discussion, it should be pointed out that spurious currents discussed in the current work only exist in the vicinity of an interface with nonzero curvature. The "spurious velocities" reported near flat interfaces [11,12] are caused by ambiguous interpretation of the true fluid velocity which by definition represents the overall momentum transfer. In typical LB simulations, the dynamics of the distribution function is split into separate streaming and collision steps. As the consequence of the long-range interaction, momentum at each lattice site changes in the collision step. The overall momentum transfer is defined by the average of the momenta before and after the collision [4]. Once the proper interpretation is used, the velocity field vanishes completely in a flat stationary interface as required by the force balance law. The pressure field is also a perfect constant once the contribution of the interaction is considered.

The presence of the anomalous circulation has caused some skepticism about the applicability of LB method in the simulation of multiphase flow. For engineering applications, the small velocities also compromises the accuracy of the numerical results, especially in situations where the detailed dynamics of the interface is of critical importance. Several attempts have been made to understand the origin and to reduce the magnitude of the spurious velocities. Wagner [13] concluded that the origin of the spurious currents are due to the incompatibility between the discretizations of the driving forces for the order parameter and momentum equation. Cristea [12] proposed a correction force term to eliminate the spurious current. In this Brief Report, we show that the origin of the spurious current in the nonideal gas LB model given in Refs. [3,4] can be understood as caused by the lack of sufficient isotropy when the gradient of the density is calculated. By adopting a finite difference gradient operator of sufficient isotropy, the spurious current can be made arbitrarily small.

We proceed by first briefly summarizing the basic algorithm of the multicomponent nonideal gas LB model [3,4]. Within the theoretical framework set forth in Ref. [14], the motion of a single component fluid system is described by a set of d discrete values of the distribution function, f_a, which obey the following lattice Bhatnagar-Gross-Krook (BGK) equation:

$$\frac{\partial f_a}{\partial t} + \boldsymbol{\xi}_a \cdot \boldsymbol{\nabla} f_a = -\frac{1}{\tau}[f_a - f_a^{(eq)}], \quad a = 1, \ldots, d, \tag{1}$$

where $\{\boldsymbol{\xi}_a\}$ is the set of abscissas of a Gauss-Hermite quadrature in the velocity space and τ the relaxation time. For the purpose of the present work, we limit the scope of our discussion to an isothermal system with unit molecular mass. The macroscopic fluid density, $\rho(\boldsymbol{x})$, and velocity, $\boldsymbol{u}(\boldsymbol{x})$, are the moments of the distribution function as the following:

$$\rho = \sum_{a=1}^{d} f_a, \quad \rho \boldsymbol{u} = \sum_{a=1}^{d} f_a \boldsymbol{\xi}_a. \tag{2}$$

The equilibrium distribution function, $f_a^{(eq)}$, is taken to be the truncated Hermite expansion of the Maxwell-Boltzmann distribution. At the second order, it is

*Electronic address: xiaowen@exa.com

$$f_a^{(eq)} = w_a \rho \left[1 + u_a + \frac{u_a^2 - u^2}{2} \right], \tag{3}$$

where $u_a \equiv \boldsymbol{u} \cdot \boldsymbol{\xi}_a$, and w_a the weight of the Gauss-Hermite quadrature associated with abscissa $\boldsymbol{\xi}_a$. Equations (1)–(3) form a closed system and exhibit the Navier-Stokes hydrodynamics with an ideal-gas equation of state at macroscopic level [1,2].

Long-range intermolecular interaction was introduced into the above system by defining a lattice version of the interaction potential between two neighboring sites $\boldsymbol{x}$ and $\boldsymbol{x}'$ [3,4]. In the single-component case it can be written as

$$V(\boldsymbol{x},\boldsymbol{x}') = G(\boldsymbol{x},\boldsymbol{x}')\psi(\boldsymbol{x})\psi(\boldsymbol{x}'), \tag{4}$$

where $G(\boldsymbol{x},\boldsymbol{x}') = G(\boldsymbol{x}-\boldsymbol{x}')$ is a Green's function and the function $\psi = \psi(\rho)$ is the "effective mass" that defines the details of the interparticle interaction. As the consequence of the interaction potential, an interaction force is induced on the particles at lattice site $\boldsymbol{x}$

$$\boldsymbol{F} = -G(|\boldsymbol{e}_a|)\psi(\boldsymbol{x}) \sum_a \psi(\boldsymbol{x} + \boldsymbol{e}_a)\boldsymbol{e}_a, \tag{5}$$

where the summation is over all neighbors interacting with $\boldsymbol{x}$. The momentum exchange so introduced among lattice sites can be easily shown to sum up to zero, which ensures exact global momentum conservation. As shown previously [14,15], a convenient and computationally efficient way to incorporate this intermolecular force into the dynamics of f_a is simply incrementing the particle momentum in $f^{(eq)}$ by the amount $\tau \boldsymbol{F}$. Namely $\boldsymbol{u}$ in Eq. (3) is replaced by $\boldsymbol{u} + \tau \boldsymbol{F}/\rho$. It is straightforward to see that the averaged momentum before and after collision is $\rho \boldsymbol{u} + \boldsymbol{F}/2$, which defines the macroscopic fluid velocity.

In its original form [3], the interaction range is defined over the nearest neighbors on a hexagonal lattice, i.e.

$$G(|\boldsymbol{e}_a|) = \begin{cases} G, & \text{if } |\boldsymbol{e}_a| = c \\ 0, & \text{if } |\boldsymbol{e}_a| > c, \end{cases} \tag{6}$$

where c is the lattice spacing. By projecting from four-dimensional (4D) FCHC lattice, the interaction was extended to the next nearest neighbors on a cubic lattice in three dimensions (3D) [16]

$$G(|\boldsymbol{e}_a|) = \begin{cases} 2G, & \text{if } |\boldsymbol{e}_a| = c \\ G, & \text{if } |\boldsymbol{e}_a| = \sqrt{2}c \\ 0, & \text{otherwise}, \end{cases} \tag{7}$$

and on a square lattice in two dimensions (2D) [17]

$$G(|\boldsymbol{e}_a|) = \begin{cases} 4G, & \text{if } |\boldsymbol{e}_a| = c \\ G, & \text{if } |\boldsymbol{e}_a| = \sqrt{2}c \\ 0, & \text{otherwise}. \end{cases} \tag{8}$$

We point out that the interaction potential can be generalized to include any number of neighbors by recognizing that the right-hand side of Eq. (5) is the finite difference representation of $-\psi \nabla \psi$ with an unspecified relative interaction strengths at different distances. The relative interaction strengths can be determined by the requirement that the finite difference gradient operator should posses sufficient degree of isotropy so as to reduce the extent of the spurious current in the vicinity of a curved interface.

Following the standard analysis procedure of finite difference schemes, we consider an arbitrary function f defined on a regular lattice. Let $\boldsymbol{x}$ be any lattice site and $\{\boldsymbol{e}_a : a = 1, \ldots, d\}$ the set of vectors pointing from $\boldsymbol{x}$ to its d neighbors. The function value at the neighboring site is given by the following Taylor series in multidimensions:

$$f(\boldsymbol{x} + \boldsymbol{e}) = \sum_{n=0}^{\infty} \frac{1}{n!} \left[\nabla^{(n)} f(\boldsymbol{x}) \right] \cdot \underbrace{\boldsymbol{e}\boldsymbol{e} \cdots \boldsymbol{e}}_{n \text{ terms}}, \tag{9}$$

where the product on the right-hand-side denotes full contraction between the two rank-n tensors. For the convenience of discussion, we follow the standard notation in Ref. [18] and write:

$$\boldsymbol{E}^{(n)}_{i_1 i_2 \ldots i_n} = \sum_a w(|\boldsymbol{e}_a|^2)(\boldsymbol{e}_a)_{i_1} \cdots (\boldsymbol{e}_a)_{i_n}, \tag{10}$$

where $w(|\boldsymbol{e}_a|^2)$ are the weights. The finite difference approximation to the gradient of f follows from Eq. (9) immediately:

$$\sum_{a=1}^{d} w(|\boldsymbol{e}_a|^2) f(\boldsymbol{x} + \boldsymbol{e}_a)\boldsymbol{e}_a = (\boldsymbol{\nabla} f) \cdot \boldsymbol{E}^{(2)} + \frac{1}{3!}(\boldsymbol{\nabla}^{(3)} f) \cdot \boldsymbol{E}^{(4)} + \frac{1}{5!}(\boldsymbol{\nabla}^{(5)} f) \cdot \boldsymbol{E}^{(6)} + \cdots . \tag{11}$$

Clearly, for the left-hand side to be a good approximation to the gradient of f, $\boldsymbol{E}^{(2)}$ must be the unit tensor. Furthermore, for any axisymmetric (2D) or spherically symmetric (3D) function, f, the gradient of f should only have the radial component. This condition is met if all the tensors $\boldsymbol{E}^{(n)}$ are isotropic. Unfortunately, with finite number of vectors in Eq. (10), only the lowest few tensors can be made isotropic by properly choosing the weights. The high-order error will *always* include an azimuthal component. In Eq. (5), the same finite difference approximation is effectively applied to the density field near a stationary drop or bubble to obtain the interaction force. The azimuthal component in the high-order terms will inevitably cause a circulation flow. In the alternative multiphase LB model of Swift *et al.* [19,20], the momentum is conserved locally at each lattice site and there is no momentum exchange. The existence of the much reduced spurious current is perhaps due to other reasons.

With a given set of vectors, it is therefore highly desirable to obtain the finite-difference gradient operator with the highest degree of isotropy. This problem is reduced to that of obtaining the weights that yield the highest isotropic $\boldsymbol{E}^{(n)}$. Reference [18] gives solutions for isotropy tensors up to $\boldsymbol{E}^{(6)}$ in both 2D and 3D. Extensions to higher orders are tedious but straightforward. Listed in Table I are solutions that yield isotropic tensors up to $\boldsymbol{E}^{(8)}$ using neighbors with components $(\boldsymbol{e}_a)_i \leqslant 2$. All solutions are scaled such that $\boldsymbol{E}^{(2)}$ equals to the unit tensor. Note that the previous results by projection from 4D FCHC as given in Eqs. (7) and (8) correspond to the solutions that yield isotropic $\boldsymbol{E}^{(4)}$.

TABLE I. Weights that yield unit $\boldsymbol{E}^{(2)}$ and isotropic $\boldsymbol{E}^{(n)}$ tensors in two and three dimensions. The tensors given in the second column is the highest isotropic $\boldsymbol{E}^{(n)}$ tensor with the corresponding weights.

	Tensor	$w(1)$	$w(2)$	$w(3)$	$w(4)$	$w(5)$	$w(6)$	$w(8)$
	$\boldsymbol{E}^{(4)}$	1/3	1/12					
2D	$\boldsymbol{E}^{(6)}$	4/15	1/10		1/120			
	$\boldsymbol{E}^{(8)}$	4/21	4/45		1/60	2/315		1/5040
	$\boldsymbol{E}^{(4)}$	1/6	1/12					
3D	$\boldsymbol{E}^{(6)}$	2/15	1/15	1/60	1/120			
	$\boldsymbol{E}^{(8)}$	4/45	1/21	2/105	5/504	1/315	1/630	1/5040

To numerically examine the effect of the isotropy of the interaction force on the spurious current, simulation of a single stationary drop was performed using the single-component nonideal gas LB model. Once the relative weights fixed, the interaction strength in Eq. (5) is controlled by a single parameter G

$$G(|\boldsymbol{e}_a|) = G \cdot w(|\boldsymbol{e}_a|^2), \tag{12}$$

which yields the following equation of state:

$$p = \rho + \frac{G}{2}\psi^2(\rho). \tag{13}$$

For simplicity, the same heuristic effective mass, $\psi(\rho)=1-\exp(-\rho/\rho_0)$ [3], is used in the present simulation. The corresponding critical point is at $G=-4$ and $\rho_0=\ln 2$. All simulation here are performed on a 100×100 square lattice with an initial drop of a radius $r_0=10$ latices located in the center of the computational domain. The interaction strength is chosen to be $G=-5$. Otherwise identical simulations are performed using the three 2D gradient operators given in Table I. Shown in Fig. 1 are the steady-state velocity field in the three cases. To illustrate the structure of the velocity field clearly, the lengths of the velocity vectors are multiplied by 100, and only the velocity field in the vicinity of the drop above a threshold of $|\boldsymbol{u}|=0.001$ is shown. To be seen is that spurious currents of eightfold symmetry present in all cases in the vicinity of the liquid-vapor interface. However, both the magnitude and the spatial extent of the spurious currents are significantly reduced as higher order isotropy is enforced in the calculation of the gradient. The maximum velocities in these three cases are also plotted in Fig. 2. By adopting an interaction rule with higher order symmetry, the spurious current can be reduced to a minimum level. Since the additional computational cost associated with the higher isotropy gradients is mainly due to the enlarged boundary range in a

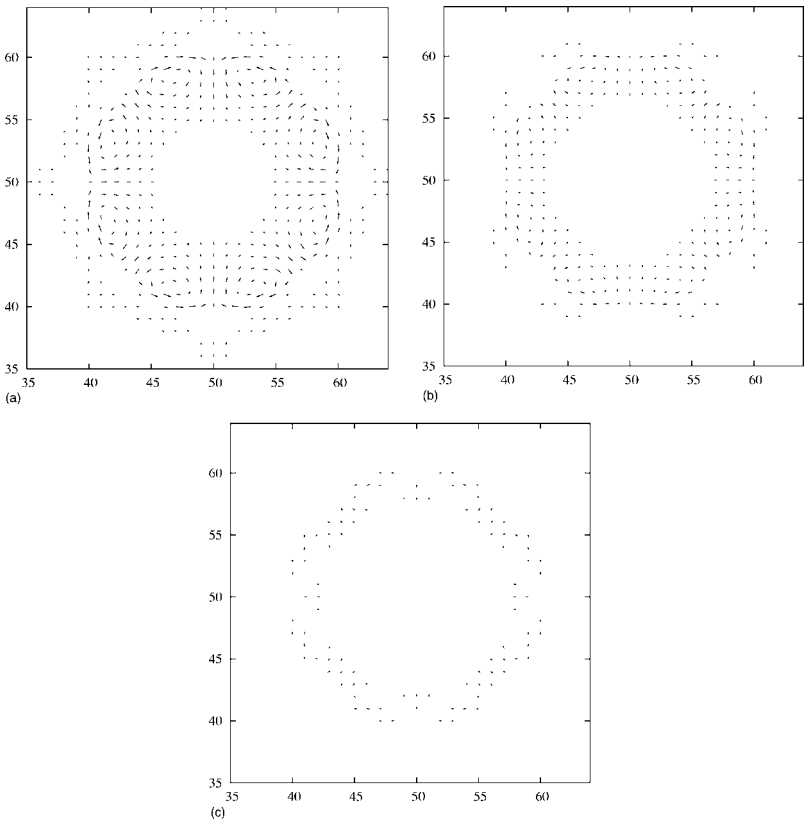

FIG. 1. Velocity distribution in the vicinity of a stationary drop. The degree of isotropy of the interaction force is 4 (a), 6 (b), and 8 (c), respectively.

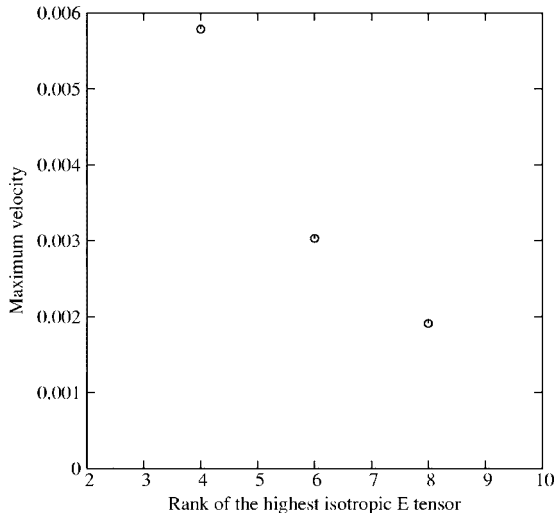

FIG. 2. The magnitude of the spurious velocity as a function of the degree of isotropy of the interaction force.

domain-decomposed distributed-memory environment, the interaction rules with the eighth order isotropy are relatively more attractive than the sixth order ones, as with the same amount of communication cost, they achieve higher degree of isotropy and smaller spurious current. In fact, these gradient operators were used in some previous simulations of multiphase flows [6,21].

A few remarks on the interaction model are called for at this point. First, although the model was originally created using mainly microscopic arguments, later analysis from the perspective of the classic continuum kinetic theory reveals that a relation can be identified between the pseudopotential ψ and the long-range intermolecular attraction and the exclusion volume of the molecules [22]. The form of ψ can be tailored to fit a fairly wide range of interaction potentials in classic kinetic theory to at least the leading order. Some high-order corrections were subsequently proposed by relaxing the exact momentum conservation and explicitly constructing the pressure tensor as functions of the derivatives of the density field according to the specification of the classic phenomenological theory [23]. However, it should be noted that substantial degree of arbitrariness can exist in the discretization of the interaction force of the continuum theory, and it is not clear whether a discrete interaction model can be so constructed without sacrificing the global momentum conservation. Second, at a further level, the lack of energy conservation in this interaction model has been recognized since its inception. The difficulty lies with both the well-known problems of the energy-conserving LB models and the construction of a discrete model with simultaneous exact conservations of global momentum and energy. Consequently, discrepancies with the predictions of classic thermodynamic theory cannot be completely precluded until full thermodynamic consistency [24,25] can be established through an explicit rigorous energy conservation relation.

In summary, the origin of the spurious circulation current in the vicinity of a curved interface between two phases is attributed to the insufficient isotropy in the calculation of density gradient. Finite difference gradient operators with higher degree of isotropy are obtained. It is numerically shown that by adopting a sufficiently isotropic gradient operator, both the magnitude and the spatial extent of the spurious current can be greatly reduced. The same technique can be applied to the multicomponent nonideal gas LB model, and other occasions where highly isotropic calculation of gradients is required.

The author thanks Dr. Hudong Chen for many helpful and intriguing discussions.

[1] S. Chen and G. Doolen, Annu. Rev. Fluid Mech. **30**, 329 (1998).
[2] S. Succi, *The Lattice Boltzmann Equation for Fluid Dynamics and Beyond*, Numerical Mathematics and Scientific Computation (Oxford University Press, New York, 2001).
[3] X. Shan and H. Chen, Phys. Rev. E **47**, 1815 (1993).
[4] X. Shan and H. Chen, Phys. Rev. E **49**, 2941 (1994).
[5] N. S. Martys and J. F. Douglas, Phys. Rev. E **63**, 031205 (2001).
[6] K. Sankaranarayanan, X. Shan, I. Kevrekidis, and S. Sundaresan, J. Fluid Mech. **452**, 61 (2002).
[7] J. Chin, E. S. Boek, and P. V. Coveney, Philos. Trans. R. Soc. London, Ser. A **360**, 547 (2002).
[8] G. Házi, A. R. Imre, G. Mayer, and I. Farkas, Ann. Nucl. Energy **29**, 1421 (2002).
[9] A. K. Gunstensen, Ph.D. thesis, MIT (1992).
[10] S. Hou, X. Shan, Q. Zou, G. D. Doolen, and W. E. Soll, J. Comp. Physiol. **138**, 695 (1997).
[11] R. R. Nourgaliev, T. N. Dinh, T. Theofanous, and D. Joseph, Int. J. Multiphase Flow **29**, 117 (2003).
[12] A. Cristea and V. Sofonea, Int. J. Mod. Phys. C **14**, 1251 (2003).
[13] A. J. Wagner, Int. J. Mod. Phys. B **17**, 193 (2003).
[14] X. Shan, X.-F. Yuan, and H. Chen, J. Fluid Mech.. **550**, 413 (2006).
[15] N. S. Martys, X. Shan, and H. Chen, Phys. Rev. E **58**, 6855 (1998).
[16] N. S. Martys and H. Chen, Phys. Rev. E **53**, 743 (1996).
[17] Q. Kang, D. Zhang, and S. Chen, Phys. Fluids **14**, 3203 (2002).
[18] S. Wolfram, J. Stat. Phys. **45**, 471 (1986).
[19] M. R. Swift, W. R. Osborn, and J. M. Yeomans, Phys. Rev. Lett. **75**, 830 (1995).
[20] M. R. Swift, E. Orlandini, W. R. Osborn, and J. M. Yeomans, Phys. Rev. E **54**, 5041 (1996).
[21] K. Sankaranarayanan, X. Shan, I. Kevrekidis, and S. Sundaresan, Chem. Eng. Sci. **54**, 4817 (1999).
[22] X. He, X. Shan, and G. Doolen, Phys. Rev. E **57**, R13 (1998).
[23] X. He and G. D. Doolen, J. Stat. Phys. **107**, 309 (2002).
[24] S. Succi, I. V. Karlin, and H. Chen, Rev. Mod. Phys. **74**, 1203 (2002).
[25] S. Ansumali and I. V. Karlin, Phys. Rev. Lett. **95**, 260605 (2005).